Effect of Functionally Graded Elastic Moduli for the Unidirectional Lamina

Nazik Khalid Hasan [1] & Saad Essa [2,3]

[1] Civil Engineering Department, Erbil Polytechnic University, Erbil, Iraq
[2] Civil Engineering Department, Erbil Polytechnic University, Erbil, Iraq
[3] Civil Engineering Department, Ishik University, Erbil, Iraq
Correspondence: Saad Essa, Ishik University, Erbil, Iraq. Email: saad.essa@ishik.edu.iq

Received: June 26, 2018 Accepted: August 25, 2018 Online Published: September 1, 2018

doi: 10.23918/eajse.v4i1sip70

Abstract: This paper is to justify the assumption feature of the functionally graded elastic moduli for both direction x-y and effect on the distribution of Poisson's ratio throughout the angle of lamina fibers between 0 to 90 degrees. In addition, the failure criterion theory is studied with consequences of the change in elasticity. Tsai-Hill failure criterion is selected in the context of unidirectional (UD) composites. The elastic changes according to natural logarithm. It reveals that the condition of closed failure envelope cannot be satisfied by all UD composites and hence the constraint should be unrestrained. The Tsai-Wu principle chiefs to that failure occur whenever the distortion yields energy equals or exceeds a certain value related to the strength of the lamina. The strains and stress for both compression and tension loading are determined based on Tsai-Hill criterion which changes with fiber orientation. The results are obtained for both stress and strains under tension and compression loading.

Keywords: Unidirectional Lamina, Lamina Fiber Angle, Orthotropic Material, Tsai-Hill Criterion

1. Introduction

The past few years have seen an extensive increase in the use of engineering processes for composite structures based on dry fiber pre-forms and different resin injection. Despite a promising number of advantages in terms of costs and flexibility of invention, such manufacturing technologies are likely to increase the density of micro-defects when compared to conventional prepreg based composite. In unidirectional (UD) composites materials, at the microscale, the stress transfer from the polymer matrix to the fiber determines the overall mechanical behavior. In addition, the matrix undergoes microstructural modifications in the vicinity of the fibers due to local changes of chemical and physical processes such as crystallization and cross-linking. The region of the matrix affected by the presence of fibers referred to as the interphase region highly affects the mechanical behavior of polymer composites.

The voids into the polymeric matrix in terms of degradation of the composite mechanical properties has been widely studied (Chowdhury, Talreja, & Benzerga, 2008) while the consequences of fiber matrix inter-facial de-cohesion are still an open issue that is receiving a great attention from the scientific community (Maligno, Warrior, & Long, 2010; Totry, Molina-Aldareguía, González, & LLorca, 2010). Numerical models have been developed by many researchers (Aghdam & Falahatgar, 2004; Asp, Berglund, & Talreja, 1996; Lane, Hayes, & Jones, 2001; Matzenmiller & Gerlach, 2005) to investigate the influence of the interphase properties on the mechanical behavior of composite

materials. The prediction of the stress in the broken fiber has been modeled by Fukuda and Kawata (1976). They have found that Young's modulus of the matrix and the fiber volume fraction had a significant influence on the magnitude of the stress concentration. Phenomenological observations of the creep rupture under maintained combined traction and torsion loading are first presented by Natalia et al. (as cited in Kotelnikova-Weiler, Baverel, Ducoulombier, & Caron, 2018). Behzadi, Curtis and Jones (2009) stablished a Monte Carlo simulation to predict the failure strain of unidirectional fiber composites. The effect of matrix shear yielding of a high-performance epoxy resin is introduced into the model through load sharing factors between the fibers adjacent to fiber-break(s). Most of the statistical models (Lienkamp, & Schwartz, 1993; Wada, & Fukuda, 1999) for composite failure strength are based on the linkage of several single fibers of the size a given ineffective length incorporated into a Monte Carlo simulation. Vanegas-Jaramillo, Turon, Costa, Cruz and Mayugo (2018) proposed that failure takes place when a critical density breaks, which depends entirely on the constituent properties. Turon et al. (2005) developed a progressive damage model for unidirectional composites laminates based on fiber fragmentation.

In this paper, the variation of elastic moduli for the graphite/epoxy composite is showed based on the Tsai-Hill criterion and obeys to the natural logarithm as shown in Figure 1. The stress and strain under the given strength properties are exhibited to identify the effect of functionally graded elastic moduli with ply-lamina angles. The $\alpha = 1$, E_1 and E_2 in GPa which refer to the longitudinal and transverse direction modulus of elasticity respectively.

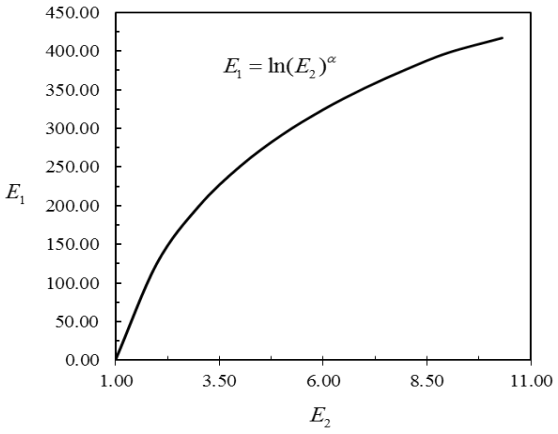

Figure 1: Variations of longitudinal and transverse elastic moduli

2. Plane Stress Assumption

A thin prismatic member can be considered as a typical lamina of plate based on plane stress assumption. This means that the plate is thin and there are no out-of-plane loads as shown in Figure 2. This assumption leads to conversion from three-dimensional stress-strain equations to two-dimensional equations.

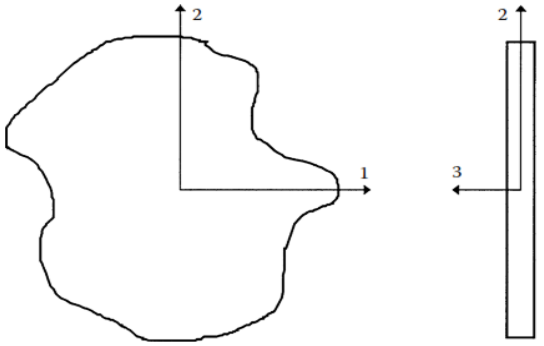

Figure 2: Plane stress conditions for thin plate

2.1 Reduction of Hooke's Law

The general strain-stress relationship for a three-dimensional body in a 1–2–3 orthogonal Cartesian coordinate system is

$$\begin{bmatrix} \varepsilon_1 \\ \varepsilon_2 \\ \varepsilon_3 \\ \gamma_{23} \\ \gamma_{31} \\ \gamma_{12} \end{bmatrix} = \begin{bmatrix} S_{11} & S_{12} & S_{13} & S_{14} & S_{15} & S_{16} \\ S_{21} & S_{22} & S_{23} & S_{24} & S_{25} & S_{26} \\ S_{31} & S_{32} & S_{33} & S_{34} & S_{35} & S_{36} \\ S_{41} & S_{42} & S_{43} & S_{44} & S_{45} & S_{46} \\ S_{51} & S_{52} & S_{53} & S_{54} & S_{55} & S_{56} \\ S_{61} & S_{62} & S_{63} & S_{64} & S_{65} & S_{66} \end{bmatrix} \begin{bmatrix} \sigma_1 \\ \sigma_2 \\ \sigma_3 \\ \tau_{23} \\ \tau_{31} \\ \tau_{12} \end{bmatrix} \tag{1}$$

In the case of anisotropic material, one finds that the compliance matrix is related directly to engineering constants as

$$\begin{aligned} S_{11} &= \frac{1}{E} = S_{22} = S_{33} \\ S_{12} &= -\frac{\nu}{E} = S_{13} = S_{21} = S_{23} = S_{31} = S_{32} \\ S_{44} &= \frac{1}{G} = S_{55} = S_{66} \end{aligned} \tag{2}$$

and S_{ij}, other than in the preceding is zero. If a material has three mutually perpendicular planes of material symmetry, then the stiffness matrix is given by

$$[C] = \begin{bmatrix} C_{11} & C_{12} & C_{13} & 0 & 0 & 0 \\ C_{12} & C_{22} & C_{23} & 0 & 0 & 0 \\ C_{13} & C_{23} & C_{33} & 0 & 0 & 0 \\ 0 & 0 & 0 & C_{44} & 0 & 0 \\ 0 & 0 & 0 & 0 & C_{55} & 0 \\ 0 & 0 & 0 & 0 & 0 & C_{66} \end{bmatrix} \tag{3}$$

Three of mutually perpendicular material with symmetric planes indicate that three mutually perpendicular planes of elastic symmetry. Nine independent elastic constants are existing. Figure 3 represents an example of orthotropic material include a single lamina of continuous fiber composite, arranged in a rectangular array, a wooden bar, and rolled steel. The compliance matrix reduces to

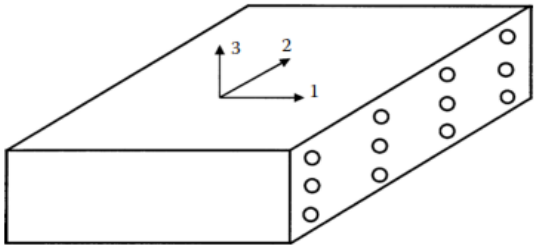

Figure 3: A unidirectional lamina as a monoclinic material with fibers

The compliance matrix reduces to

$$[S]=\begin{bmatrix} S_{11} & S_{12} & S_{13} & 0 & 0 & 0 \\ S_{12} & S_{22} & S_{23} & 0 & 0 & 0 \\ S_{13} & S_{23} & S_{33} & 0 & 0 & 0 \\ 0 & 0 & 0 & S_{44} & 0 & 0 \\ 0 & 0 & 0 & 0 & S_{55} & 0 \\ 0 & 0 & 0 & 0 & 0 & S_{66} \end{bmatrix} \tag{4}$$

A unidirectional lamina falls under the orthotropic material category. If the lamina is thin also does not carry any out-of-plane loads, one can assume plane stress conditions for the lamina. By taking Eq. (1) and Eq. (4) and assuming $\sigma_3 = 0$, $\tau_{23} = 0$ and $\tau_{31} = 0$, then

$$\begin{aligned} \varepsilon_3 &= S_{13}\sigma_1 + S_{23}\sigma_2 \\ \gamma_{23} &= \gamma_{31} = 0 \end{aligned} \tag{5}$$

Eq. (4) for an orthotropic plane stress problem can be written as

$$\begin{bmatrix} \varepsilon_1 \\ \varepsilon_2 \\ \gamma_{12} \end{bmatrix} = \begin{bmatrix} S_{11} & S_{12} & 0 \\ S_{12} & S_{22} & 0 \\ 0 & 0 & S_{66} \end{bmatrix} \begin{bmatrix} \sigma_1 \\ \sigma_2 \\ \tau_{12} \end{bmatrix} \tag{6}$$

where S_{ij} are the elements of the compliance matrix with the four independent compliance elements. Inverting Eq. (6) gives the stress-strain relationship as

$$\begin{bmatrix} \sigma_1 \\ \sigma_2 \\ \tau_{12} \end{bmatrix} = \begin{bmatrix} Q_{11} & Q_{12} & 0 \\ Q_{12} & Q_{22} & 0 \\ 0 & 0 & Q_{66} \end{bmatrix} \begin{bmatrix} \varepsilon_1 \\ \varepsilon_2 \\ \gamma_{12} \end{bmatrix} \tag{7}$$

where Q_{ij} are the reduced stiffness coefficients, which are related to the compliance coefficients as

$$Q_{11} = \frac{S_{22}}{S_{11}S_{22} - S_{12}^2}$$
$$Q_{12} = -\frac{S_{12}}{S_{11}S_{22} - S_{12}^2} \quad (8)$$
$$Q_{22} = \frac{S_{11}}{S_{11}S_{22} - S_{12}^2}$$
$$Q_{66} = \frac{1}{S_{66}}$$

2.2 Relationship of Compliance and Stiffness Matrix to Elastic Constants of Lamina

Eq. (6) and Eq. (7) show the relationship of stress and strain through the compliance $[S]$ and reduced stiffness $[Q]$ matrices. On the other hand, stress and strains are generally related to engineering elastic constants. For a unidirectional lamina, these engineering elastics constants are

E_1 = longitudinal Young's modulus (in direction 1)

E_2 = transverse Young's modulus (in direction 2)

ν_{12} = major Poisson's ratio, where the general Poisson's ratio, ν_{ij} is defined as the ratio of the negative of the normal strain in the direction j to the normal strain in direction i, when the only normal load is applied in direction i.

G_{12} = in-plane shear modulus (in plane 1–2)

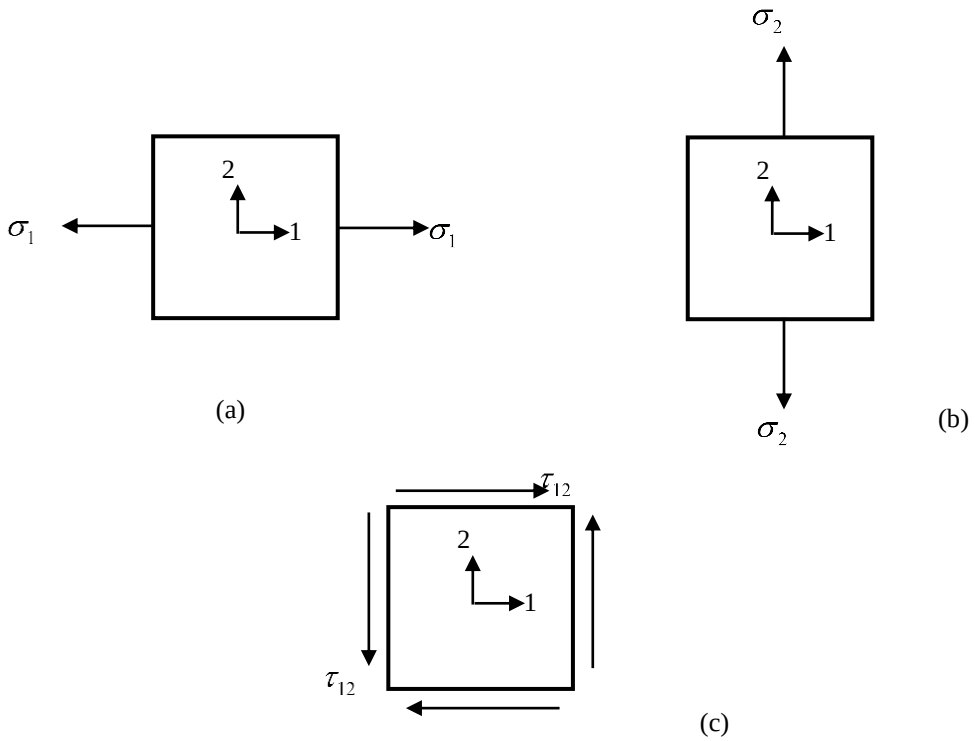

Figure 4: Application of stresses of unidirectional lamina

The Figure (4a) is representing an application of a pure tensile, that is

$$\sigma_1 \neq 0, \sigma_2 = 0, \tau_{12} = 0 \tag{9}$$

Then, from Eq. (6)

$$\begin{aligned} \varepsilon_1 &= S_{11}\sigma_1 \\ \varepsilon_2 &= S_{12}\sigma_1 \\ \gamma_{12} &= 0 \end{aligned} \tag{10}$$

With the only nonzero stress is σ1, as is the case here, then

$$E_1 \equiv \frac{\sigma_1}{\varepsilon_1} = \frac{1}{S_{11}} \tag{11}$$

$$\nu_{12} \equiv -\frac{\varepsilon_2}{\varepsilon_1} = -\frac{S_{12}}{S_{11}} \tag{12}$$

For the pure tensile load application in direction 2 as shown in Figure (4b), that is

$$\sigma_1 = 0, \sigma_2 \neq 0, \tau_{12} = 0 \tag{13}$$

Then, from Eq. (6)

$$\begin{aligned} \varepsilon_1 &= S_{12}\sigma_2 \\ \varepsilon_2 &= S_{22}\sigma_2 \\ \gamma_{12} &= 0 \end{aligned} \tag{14}$$

If the only nonzero stress is σ_2 , as is the case here, then

$$E_2 \equiv \frac{\sigma_2}{\varepsilon_2} = \frac{1}{S_{22}} \tag{15}$$

$$\nu_{21} \equiv -\frac{\varepsilon_1}{\varepsilon_2} = -\frac{S_{12}}{S_{22}} \tag{16}$$

The ν_{21} is the minor Poisson's ratio. From Eq. (11), Eq. (12), Eq. (15) and Eq. (16), the reciprocal relationship

$$\frac{\nu_{12}}{E_1} = \frac{\nu_{21}}{E_2} \tag{17}$$

With applying a pure shear stress in the plane 1–2 as shown in Figure (4c), that is,

$$\sigma_1 = 0, \sigma_2 = 0, \tau_{12} \neq 0 \tag{18}$$

Then, from Eq. (6)

$$\begin{aligned} \varepsilon_1 &= 0 \\ \varepsilon_2 &= 0 \\ \gamma_{12} &= S_{66}\tau_{12} \end{aligned} \tag{19}$$

In condition, τ_{12} is the only nonzero stress, as is the case here, then

$$G_{12} \equiv \frac{\tau_{12}}{\gamma_{12}} = \frac{1}{S_{66}} \tag{20}$$

Thus,

$$\begin{aligned} S_{11} &= \frac{1}{E_1} \quad , \quad S_{12} = -\frac{\nu_{12}}{E_1} \\ S_{22} &= \frac{1}{E_2} \quad , \quad S_{66} = \frac{1}{G_{12}} \end{aligned} \tag{21}$$

Also, the stiffness coefficients Q_{ij} are related to the engineering constants through Eq. (8) and Eq. (21) as

$$\begin{aligned} Q_{11} &= \frac{E_1}{1-\nu_{21}\nu_{12}} \quad , \quad Q_{12} = \frac{\nu_{12}\, E_2}{1-\nu_{21}\nu_{12}} \\ Q_{22} &= \frac{E_2}{1-\nu_{21}\nu_{12}} \quad , \quad Q_{66} = G_{12} \end{aligned} \tag{22}$$

3. Tsai-Hill Failure Theory

This theory is based on the distortion energy failure theory of Von-Mises' distortion energy yield criterion for isotropic materials as applied to anisotropic materials. Distortion energy is actually a part of the total strain energy in a body. The strain energy in a body consists of two parts; one due to a change in volume and is called the dilation energy and the second is due to a change in shape and is called the distortion energy. It is assumed that failure in the material takes place only when the distortion energy is greater than the failure distortion energy of the material. Hill adopted the Von-Mises' distortion energy yield criterion to anisotropic materials. Then, Tsai adapted it to a unidirectional lamina. Based on the distortion energy theory, he proposed that a lamina has failed if

$$\begin{aligned} &\left(G_2+G_3\right)\sigma_1^2+\left(G_1+G_3\right)\sigma_2^2+\left(G_1+G_2\right)\sigma_3^2-2G_3\sigma_1\sigma_2-2G_2\sigma_1\sigma_3 \\ &-2G_1\sigma_2\sigma_3+2G_4\tau_{23}^2+2G_5\tau_{13}^2+2G_6\tau_{12}^2<1 \end{aligned} \tag{23}$$

is violated. The components G_1, G_2, G_3, G_4, G_5 and G_6 of the strength criterion depend on the failure strengths and are found as follows.

Case I: The lamina will fail if apply $\sigma_1 = \left(\sigma_1^T\right)_{ult}$ to a unidirectional lamina. Eq. (23) reduces to

$$\left(G_2+G_3\right)\left(\sigma_1^T\right)_{ult}^2 = 1 \tag{24}$$

Case II: The lamina will fail if apply $\sigma_2 = \left(\sigma_2^T\right)_{ult}$ to a unidirectional lamina. Eq. (23) reduces to

$$\left(G_1+G_3\right)\left(\sigma_2^T\right)_{ult}^2 = 1 \tag{25}$$

Case III: The lamina will fail if apply $\sigma_3 = \left(\sigma_2^T\right)_{ult}$ to a unidirectional lamina and assuming that the normal tensile failure strength is same in directions (2) and (3). Thus, Eq. (23) reduces to

From Equation (2.145) to Equation (2.148), $\left(G_1 + G_2\right)\left(\sigma_2^T\right)_{ult}^2 = 1$ (26)

Case IV: The lamina will fail if apply $\tau_{12} = \left(\tau_{12}\right)_{ult}$ to a unidirectional lamina. Eq. (23) reduces to

$$2G_6\left(\tau_{12}\right)_{ult}^2 = 1 \tag{27}$$

From Eq. (24) to Eq. (27)

$$G_1 = \frac{1}{2}\left(\frac{2}{\left[\left(\sigma_2^T\right)_{ult}\right]^2} - \frac{1}{\left[\left(\sigma_1^T\right)_{ult}\right]^2}\right),\ G_2 = \frac{1}{2}\left(\frac{1}{\left[\left(\sigma_1^T\right)_{ult}\right]^2}\right) \tag{28}$$

$$G_3 = \frac{1}{2}\left(\frac{1}{\left[\left(\sigma_1^T\right)_{ult}\right]^2}\right),\ G_6 = \frac{1}{2}\left(\frac{1}{\left[\left(\tau_{12}\right)_{ult}\right]^2}\right)$$

Because the unidirectional lamina is assumed to be under plane stress, that is, then $\sigma_3 = \tau_{31} = \tau_{23} = 0$, then Eq. (23) reduces through Eq. (28) to

$$\left[\frac{\sigma_1}{\left(\sigma_1^T\right)_{ult}}\right]^2 - \left[\frac{\sigma_1\sigma_2}{\left(\sigma_1^T\right)_{ult}^2}\right] + \left[\frac{\sigma_2}{\left(\sigma_2^T\right)_{ult}}\right]^2 + \left[\frac{\tau_{12}}{\left(\tau_{12}\right)_{ult}}\right]^2 < 1 \tag{29}$$

4. Numerical Example

The aim of this part is to find the engineering constants based on combination of Elastic moduli in both direction 1 and 2 according to these criteria, Poisson's ratio: 0.28, shear modulus: 7.17 and angle of lamina: 40.6. While the elastic moduli will be like this, longitudinal elastic modulus: 181(GPa) times natural logarithm of transverse elastic modulus or in the other words equal to $181\times\ln(10.3)$. Also, the value of transverse elastic modulus: 10.3(GPa) times natural logarithm of longitudinal elastic modulus or equal to $10.3\times\ln(181)$. Ultimate longitudinal tensile strength $=1.5\text{GPa}$, ultimate longitudinal compressive strength $=-1.5\text{GPa}$, ultimate transverse tensile strength $=40\text{MPa}$, ultimate transverse compressive strength $=-246\text{MPa}$, and ultimate in-plane shear strength $=68\text{MPa}$. Transverse global strain $=\text{-}1.238\times10^{-8}$, longitudinal global strain $=4.42\times10^{-8}$, in-plane global strain $=0$. The results appear like in the Table 1 at the angle of fiber $40.6°$.

Table 1: The results at the lamina angle $40.6°$

E_x	26.4099 GPa
E_y	24.7774 GPa
G_{xy}	39.8211 GPa
ν	0.772562
shear coupling x	7.1377
shear coupling y	-0.335251

The distribution of x-direction elastic moduli or E_1 and y-direction is summarized in Table 2.

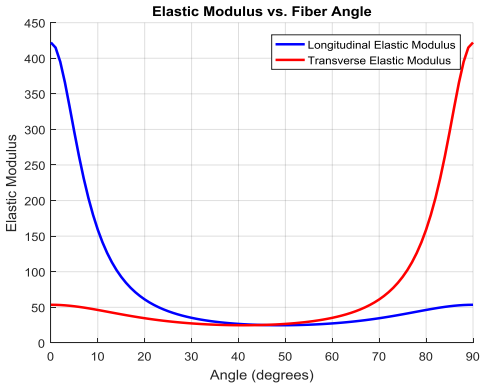

Figure 5: Functionally graded elastic modulus as a function of angle of lamina.

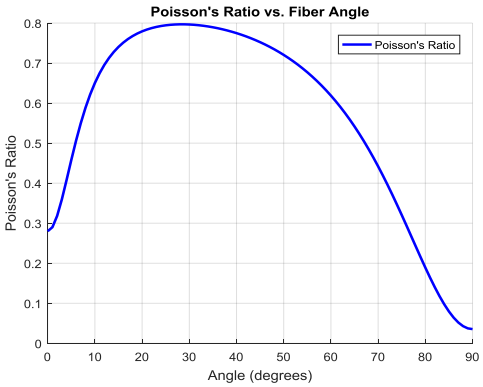

Figure 6: Poisson's ratio ν_{xy} as a function of angle of lamina for a graphite/epoxy lamina.

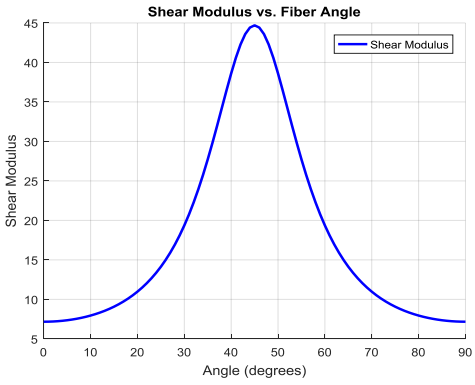

Figure 7: In-plane shear modulus in xy-plane as a function of angle of lamina for a graphite/epoxy lamina.

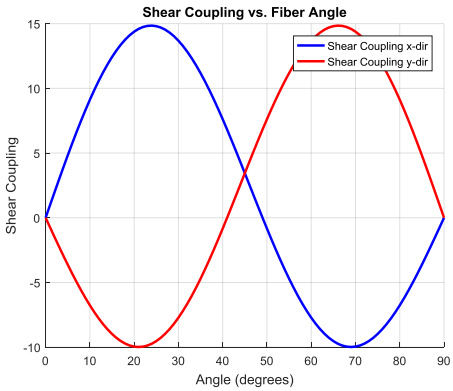

Figure 8: Shear coupling coefficients as a function of angle of lamina for a graphite/epoxy lamina.

Table 2: Variations of Functionally graded elastic moduli for both directions

Angle	E_1	E_2
0	422.1180	53.5445
10	159.1000	46.2770
20	61.0790	34.6450
30	35.2090	27.3560
45	25.1270	25.1270
90	53.5450	422.1200

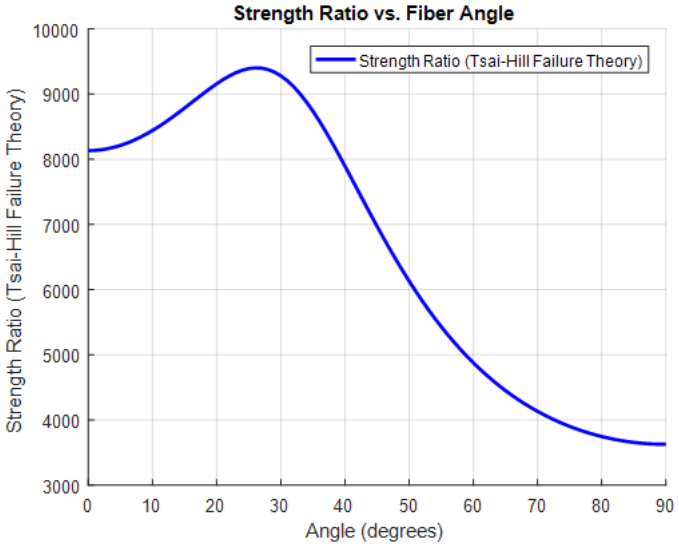

Figure 9: strength ratio for a unidirectional lamina based on Tsai-Hill failure theory

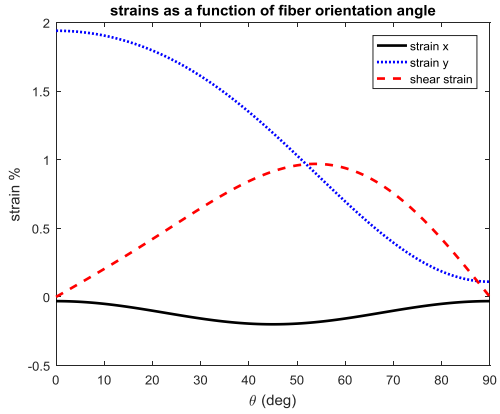

Figure 10: percentage in-plane strains as a function of fiber orientation

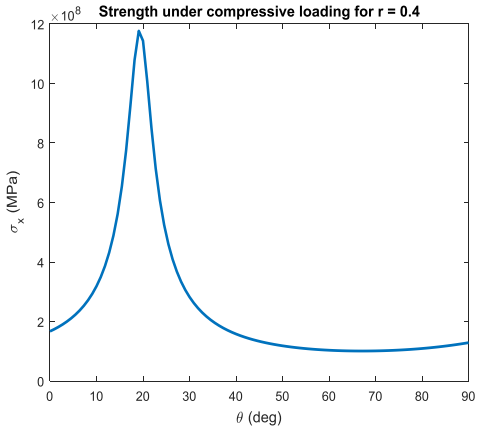

Figure 11: Distribution of strength of this layer based on Tsai-Hill criterion as a function of the fiber orientation under compression loading.

The strain and stress distribution of graphite/epoxy for both tensile and compression loading are shown in Figures 10 and 11 respectively. The strength properties of graphite/epoxy are assumed:

$$X_t = 1260\,\text{MPa}\ ,\ X_c = 2500\,\text{MPa}\ ,\ Y_t = 61\text{MPa}\ ,\ Y_c = 202\,\text{MPa}\ ,\ S = 67\,\text{MPa}$$

In addition, the individual ply thickness $= 0.00125m$ and $r = \dfrac{\sigma_y}{\sigma_x} = 0.4$

The denotation of t refers to the tension and c refers to the compression. This means that the $\left(\sigma_1^T\right)_{ult} = X_t$, $\left(\sigma_2^T\right)_{ult} = Y_t$ and $\left(\tau_{12}\right)_{ult} = S$ for the calculating of tension strength and same procedures for the compression strength. Also, the Figure 11 illustrates the strength of the layer under tensile strength based on Tsai-Hill criterion.

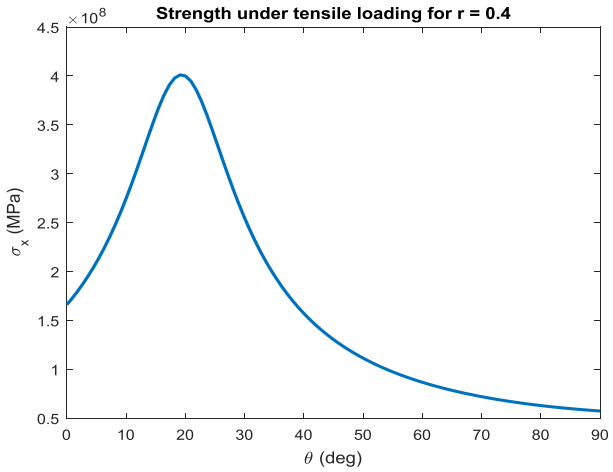

Figure 11: Distribution of strength of this layer based on the Tsai-Hill criterion as a function of the fiber orientation under tensile loading.

5. Conclusion

Applying model Figure 1 for the carbon fibers embedded in an epoxy matrix to signify the distribution of elastic moduli and Poisson's ratio within the composite and fiber orientation angle. Figure 5 shows that the elastic modulus distribution with the angle of lamina fibers. The longitudinal elastic modulus step decreasing in its values with increasing the angle of lamina fiber between $0°$ to $40°$ then increases gradually till the end of the angle of fiber. While in the transverse elastic modulus it starts from 53.545 GPa and slightly decreasing up to $40°$ then increases steeply to 422.12 GPa at the end of the lamina. Table 2 shows that the elastic moduli at angle 0 for x-direction equal to the elastic moduli at the angle of 90 for y-direction and vice versa. Poisson's ratio increases from 0.28 to 0.7968 at $28°$ of angle lamina fiber then decreases to 0.035517 at $90°$. Regards to Tsai-Hill criterion of failure, Figure 9 demonstrates the maximum strength ratio 9400 at the angle $27°$ then decrease to 3628 at the angle of lamina fiber $90°$. This means that the strength is not maximum at the start or end point but it varies throughout the lamina. The strain in y-direction decreases while the x-direction strain remains about 0 at start and end points despite at the angle $45°$ goes down.

The progression can be developed to structures subjected to non-homogeneous stresses where both ply-by-ply and point-to-point strength analyses are gradually applied. This criterion failure theory is only as good as the data available. The failure criterion is only the base for the combined stresses where data are unavailable.

References

Aghdam, M. M., & Falahatgar, S. R. (2004). Micromechanical modeling of interface damage of metal matrix composites subjected to transverse loading. *Composite Structures*, *66*(1-4), 415-420.

Asp, L. E., Berglund, L. A., & Talreja, R. (1996). Effects of fiber and interphase on matrix-initiated transverse failure in polymer composites. *Composites Science and Technology*, *56*(6), 657-

665.

Behzadi, S., Curtis, P. T., & Jones, F. R. (2009). Improving the prediction of tensile failure in unidirectional fibre composites by introducing matrix shear yielding. *Composites Science and Technology*, *69*(14), 2421-2427.

Chowdhury, K. A., Talreja, R., & Benzerga, A. A. (2008). Effects of manufacturing-induced voids on local failure in polymer-based composites. *Journal of Engineering Materials and Technology*, *130*(2), 021010.

Fukuda, H., & Kawata, K. (1976). On the stress concentration factor in fibrous composites. *Fibre Science and Technology*, *9*(3), 189-203.

Kotelnikova-Weiler, N., Baverel, O., Ducoulombier, N., & Caron, J. F. (2018). Progressive damage of a unidirectional composite with a viscoelastic matrix, observations and modelling. *Composite Structures*, *188*, 297-312.

Lane, R., Hayes, S. A., & Jones, F. R. (2001). Fibre/matrix stress transfer through a discrete interphase: 2. High volume fraction systems. *Composites science and technology*, *61*(4), 565-578.

Lienkamp, M., & Schwartz, P. (1993). A Monte Carlo simulation of the failure of a seven fiber microcomposite. *Composites science and technology*, *46*(2), 139-146.

Maligno, A. R., Warrior, N. A., & Long, A. C. (2010). Effects of interphase material properties in unidirectional fiber reinforced composites. *Composites Science and Technology*, *70*(1), 36-44.

Matzenmiller, A., & Gerlach, S. (2005). Parameter identification of elastic interphase properties in fiber composites. *Composites Part B: Engineering*, *37*(2-3), 117-126.

Totry, E., Molina-Aldareguía, J. M., González, C., & LLorca, J. (2010). Effect of fiber, matrix and interface properties on the in-plane shear deformation of carbon-fiber-reinforced composites. *Composites Science and Technology*, *70*(6), 970-980.

Turon, A., Costa, J., Maimi, P., Trias, D., & Mayugo, J. A. (2005). A progressive damage model for unidirectional fibre-reinforced composites based on fibre fragmentation. Part I: Formulation. *Composites Science and Technology*, *65*(13), 2039-2048.

Vanegas-Jaramillo, J. D., Turon, A., Costa, J., Cruz, L. J., & Mayugo, J. A. (2018). Analytical model for predicting the tensile strength of unidirectional composites based on the density of fiber breaks. *Composites Part B: Engineering*, *141*, 84-91.

Wada, A., & Fukuda, H. (1999). Approximate upper and lower bounds for the strength of unidirectional composites. *Composites Science and Technology*, *59*(1), 89-96.